Studies of boron–interstitial clusters in Si

2003 J. Phys.: Condens. Matter 15 4967

(http://iopscience.iop.org/0953-8984/15/29/308)

INSTITUTE OF PHYSICS PUBLISHING JOURNAL OF PHYSICS: CONDENSED MATTER

J. Phys.: Condens. Matter **15** (2003) 4967–4977 PII: S0953-8984(03)62249-6

Studies of boron–interstitial clusters in Si

Peter Deák[1,4], Adam Gali[1], András Sólyom[1], Pablo Ordejón[2], Katalin Kamarás[3] and Gabor Battistig[4]

[1] Budapest University of Technology and Economics, Department of Atomic Physics, Budafoki út 8, H-1111 Budapest, Hungary
[2] Institut de Ciencia de Materials de Barcelona, E-08193 Bellaterra, Barcelona, Spain
[3] Research Institute for Solid State Physics and Optics, Hungarian Academy of Science, H-1128 Budapest, Hungary
[4] Research Institute for Technical Physics and Materials Science, Hungarian Academy of Science, H-1128 Budapest, Hungary

E-mail: p.deak@eik.bme.hu

Received 15 April 2003
Published 11 July 2003
Online at stacks.iop.org/JPhysCM/15/4967

Abstract

The large number of self-interstitials created during implantation mediate the fast transient diffusion of implanted boron, leading to clustering. Sophisticated annealing strategies based on knowledge of the formation energy of the clusters are required to achieve full activation of the implant. In recent years attempts have been made to determine these data *a priori* from theoretical calculations. However, energy calculations alone are not sufficient to establish the key players in the clustering process of boron. The present paper describes a systematic first-principles quantum mechanical study of the characteristic vibration frequencies of a large number of boron–interstitial clusters (including possible configurational isomers). Comparison with the first Raman spectra obtained on B-implanted samples after high temperature annealing is presented.

(Some figures in this article are in colour only in the electronic version)

1. Introduction

Defect engineering is a key part of microelectronic device processing. Tight control of the doping requires detailed knowledge about the incorporation and activation of the dopants as well as about the influence of intrinsic defects and impurities. One of the main concerns in implantation doping and subsequent annealing is the formation of complexes. Dopant–dopant or dopant–defect complexes diminish the activation rate while defect–defect complexes may act as traps, again reducing the free carrier concentration. Identification of the most likely complexes might help in designing successful annealing strategies to get rid of these effects. An effective way to do this is the comparison of calculated spectroscopic properties of a variety of complexes with experimentally observed centres. Such a study is described here for boron–interstitial clusters (BICs) in silicon.

BICs are known to be a key problem in controlling diffusion and activation of ultra-shallow boron implants in ULSI silicon device technology. During post-implantation annealing the self-interstitials, which had been created by radiation damage, mediate fast transient diffusion of boron, during which stable and metastable BICs are formed. The BICs are either electrically inactive or the number of holes they can provide per number of boron atoms is significantly less than one. This causes a significant decrease in the activation rate. Therefore, sophisticated annealing strategies have to be developed to regain isolated boron substitutionals from BICs.

The standard approach for studying the deactivation of boron due to clustering is to try to elucidate defect properties from comparison of SIMS diffusion profiles and spreading resistance profiles. While the formation and dissolution energies of the possible clusters have been obtained previously as fitting parameters of kinetic models (see, e.g., [1]), in recent years attempts have been made to determine these data *a priori* from first-principles theoretical calculations [2–4]. For that purpose 'wholesale' calculations have been carried out on a large number of different BICs consisting of up to 8 or more boron and self-interstitial atoms. The deviation of the calculated values from the fitted ones is generally about 25% [4] but differs substantially (sometimes by 100%) from one calculation to another on the same cluster, even if the same method (actually the same computer code) was used [2, 4]. The reason is the inherent uncertainty of the applied corrections to density functional theory (DFT) and the supercell approach which are used to predict the energetics of defects [5]. There are even differences in the predicted transformations of the simplest cluster, BI, during diffusion [6–8]. Calculations also predict the dominance of 'pure' B clusters after annealing at about 800 °C, while parametric models [9, 10] emphasize clusters with an equal number of B's and I's. DFT calculations are regarded as superior to empirical tight binding ones even though (unlike the latter [11]) they predict complexes of substitutional B atoms to be energetically unfavourable, despite the fact that the calculated vibration modes of B_{Si}–B_{Si} could have been identified with bands of the boron-related infrared (IR) spectrum in silicon [12].

Apparently, energy calculations alone are not sufficient to establish the key players in the clustering process of boron. An alternative strategy would be to identify the most important BICs based on their spectroscopic properties. For that purpose, comparison of the calculated properties of BICs with the IR and Raman spectra as well as with the deep level transient spectroscopy (DLTS) spectra of B-implanted samples at various stages of annealing is necessary. Apart from early studies on the substitutional B, and the B + I and B + B pairs (see [13–15] and references therein), no report of such investigations can be found in the literature. A single (combined) study was reported in 1993 [16] leading to the establishment of a 12-atom boron cluster [17] in as-implanted samples.

The present study describes systematic first-principles quantum mechanical calculations of the characteristic vibration frequencies of all the BICs which have been suggested so far to be important in the de/reactivation process of boron. Figure 1 shows the BICs selected to be the subjects of the first series of calculations from the list published in [4]. In addition, some isomers of these BICs have also been studied. Study of the remaining possible complexes as well as the calculation of the electronic levels is in progress.

The usual nomenclature of BICs, B_nI_m, is based on the number n of boron atoms and the number m of interstitials involved in the cluster, irrespective of the fact that the interstitial can be boron or a silicon atom. In this notation, BI may equally mean an interstitial boron or a silicon self-interstitial next to a substitutional boron. Such systems are configurational isomers with the same number of atoms. In order to be able to differentiate among the possible isomers the present study uses the notations Si_i, B_i and B_s for interstitial silicon and boron, and for substitutional boron, respectively.

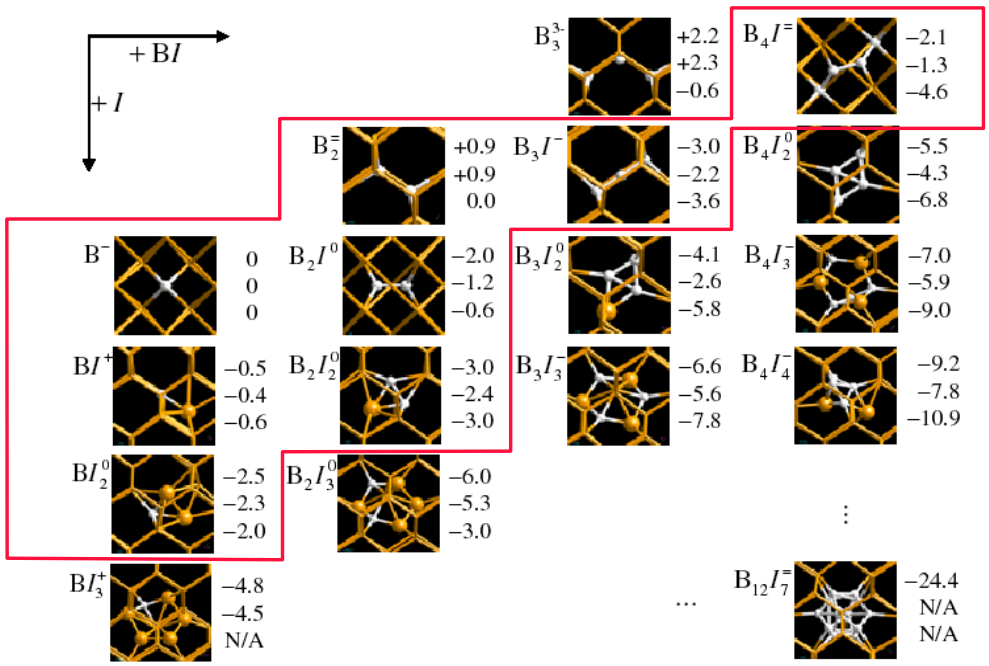

Figure 1. Structure and energetics of the BICs considered by Windl *et al* [4]. The small white balls are B atoms and the large balls are Si atoms involved in the cluster. All other Si atoms are shown as a stick-only network. The energy values (eV) next to each picture are, from top to bottom, corrected formation energies from GGA, LDA and the fitted values from [1]. The BICs marked by the polygon have been considered in this study.

2. Methods

First-principles supercell calculations have been carried out using the SIESTA code [18]. SIESTA implements DFT combined with the pseudopotential approximation, and uses numerical atomic orbitals as a basis set. It is aimed at large-scale calculations with linear-scaling simulations but is also capable of employing conventional diagonalization methods. In this work, only the latter capability was used. Norm-conserving pseudopotentials have been generated according to the Troullier–Martins [19] scheme, in the Kleinman–Bylander [20] separable form. Core radii of 1.78 and 1.89 bohr were used for B and Si, respectively. The program requires the use of a grid to compute some of the contributions to the matrix elements and total energy, and also for performing the Fourier transforms needed to evaluate the Hartree potential and energy by solving Poisson's equation in reciprocal space. A grid fine enough to represent plane waves with kinetic energy up to 90 Ryd has been used. The calculations were carried out using the generalized gradient approximation (GGA) with the Perdew–Burke–Ernzerhof functional [21]. A high quality basis set was used, consisting of double-ζ plus polarization functions for the valence electrons of all atom types. The maximum extent of these functions was 5.965 Å. Structural relaxation was performed by means of the conjugated gradient algorithm until the forces were smaller than 0.04 eV Å^{-1}. To obtain the vibrational normal modes in the harmonic approximation, the second derivative of the total energy has been calculated by means of finite differences. Since these are the only values of interest, the total energy has not been corrected either for the DFT gap error or for the supercell dispersion error. Due to the same reason, no charge correction has been applied either.

Table 1. Comparison of BIC formation energies obtained with different supercells and MP sets within the GGA approximation. The values contain no corrections (those of Windl *et al* have been obtained from figure 1 by subtracting the charge correction). The formation energies of Si_i(I) and B_s^- (B^-) have been calculated with respect to the chemical potential of the bulk materials, while those of all other complexes are with respect to I and B^-. Note the positive formation energy of B_2^-. (Note that, in agreement with earlier first-principles calculations [4, 12], $(B_s)_2$ has been found to be metastable with respect to two isolated B_s. Increasing the cell size does not help that.)

	Present		Reference [4]	Present	
BIC	64-atom cell 1^3 MP set	64-atom cell 2^3 MP set	64-atom cell, 4^3 MP set	216-atom cell 2^3 MP set	216-atom cell 1^3 MP set
I	2.53	3.65		3.61	3.35
B^-	$-\mu_B - 80.33$	$-\mu_B - 80.46$		$-\mu_B - 80.53$	$-\mu_B - 80.50$
BI^+	−0.24	−0.69	**−0.5**		−0.42
BI_2	−2.14	−2.30	**−2.4**		
B_2^{2-}	+0.87	+0.76	**+0.9**		+0.88
B_2I	−1.07	−1.71	**−1.7**		−1.44
B_2I_2	−1.98	−2.74	**−2.7**	−2.53	−2.35
B_3I^-	−1.98	−2.67	**−2.7**		−2.30
B_4I^{2-}	−1.31	−1.92	**−2.1**	−1.66	−1.53

The vibration calculations are computationally very demanding even using supercomputers. In order to keep the usage of resources within the available framework without compromising the predictive power of the results, careful convergence tests had to be carried out. First, the effect of the size of the supercell and of the quality of the Brillouin zone (BZ) summation had to be checked. BZ summations in supercell calculations are usually replaced by a weighted sum over a representative Monkhorst–Pack (MP) k-point set [22]. The formation energies in figure 1 have been obtained by Windl *et al* [4] on a 64-atom supercell in a plane wave supercell calculation using ultrasoft pseudopotentials and a 4^3 MP set (these values also contain a charge correction). Table 1 shows SIESTA results in comparison.

As can be seen, formation energies, obtained with the 2^3 MP set in the 64-atom unit cell, are within 0.2 eV of those of the 4^3 set. This justifies restriction to the 2^3 set, leading to a factor of 2–16 (depending on the symmetry of the BIC) saving in computational resources. Tests with the 216-atom cell show that the effect of the appropriate BZ summation is much more significant than that of the size of the unit cell, justifying the use of the 64-atom cell. Note that the divacancy in silicon has been regarded as a worst case test where the correct configuration of the defect could only be obtained with more than 200 atoms in a molecular cluster calculation [23]. Our 216-atom, single-k-point supercell calculation reproduces the large pairing distortion of the neighbours of the divacancy, and the geometry does not change essentially in a 512- or a 1000-atom supercell. The fact that the geometry itself does not change more than 0.01 Å between the 64- and 216-atom calculations for these BICs ensures that the calculated vibration frequencies are close to convergence.

In fact the geometry is much less sensitive to the BZ summation than the formation energy, so the question arises whether the 1^3 set (Γ point approximation) would not suffice for vibration calculations. An additional parameter for the latter is the number of atoms which are allowed to vibrate in the frozen framework of the rest. For localized vibration modes (LVMs) with frequencies well apart from the phonon continuum it is usually sufficient to consider the vibrations of those atoms only which belong directly to the defect cluster. Since many of the normal modes of the BICs are expected to be close to the Raman frequency of Si (520 cm^{-1}), a stronger mixture of the LVMs with the continuum modes might occur. Table 2 shows results obtained by allowing different numbers of shells around the complex to vibrate.

Table 2. Comparison ^{11}B vibration frequencies (cm^{-1}) calculated by allowing a different number of next-neighbour (NN) shells around the complex to vibrate.

BIC	64, 1^3 MP all atoms vibrating	64, 1^3 MP 3 NNs vibrating	64, 1^3 MP 2 NNs vibrating	64, 2^3 MP 2 NNs vibrating
B_s^-	610	609	610	**607**
B_2^{2-}	618		618	**627**
	590		589	**577**
B_2I_2		880	880	**926**
		669	670	**684**
		575	576	**565**
		556	554	**539**
B_4I^{2-} (C_{2v})		961	961	**1019**
		771	771	**744**
		727	729	**730**
		655	657	**652**
		643	642	**641**
		606	607	**609**

As can be seen, the restriction to second-neighbour shell (2NN) provides sufficiently convergent results even for the lowest LVMs. On the other hand, the use of the 2^3 MP set for the vibration calculation seems unavoidable.

As a result of the convergence tests, the following calculations have been carried out on the 64-atom cell with the 2^3 MP set and 2NN shells vibrating. This is more or less what we can afford to do at most, considering the large number of complexes we have to investigate. The tests above provide a basis to judge the convergence of the results. According to earlier experience, the typical accuracy of such calculated vibration frequencies is about ± 30 cm^{-1}. The substitutional boron acceptor has an experimentally well established LVM at 623 cm^{-1} (see section 4), to be compared with our prediction of 607 cm^{-1}.

3. Results

In table 3 the calculated vibration frequencies of the BIC-related LVMs are given, assuming the presence of either only ^{11}B or only ^{10}B (the latter values in parentheses).

From the two possible isomers of BI, B_i does not give rise to LVMs above the phonon continuum. Even though B_2, alias $(B_s)_2$, appears to be metastable with respect to two isolated B_s atoms, it might be created in the dissolution process of larger BICs. It has a double acceptor level above that of the single boron acceptor. Therefore both the neutral and the double negative charge state has been calculated, where the former should occur in p-type (where the level of boron activation is high) and the latter in compensated samples (or where the activation level of boron is low). Among the possible isomers of B2I the following were considered: the boron pair splitting a substitutional site in a [001] dumbbell configuration and two B_s on neighbouring sites with a Si_i between them (D_{3d} in the neutral, and a puckered C_{1h} symmetry in the doubly negative charge state). Further $2B_s + Si_i$ complexes are possible in other charge states. $(B_2)_s^0$ is more stable than $(B_s–Si_i–B_s)^0$ by 0.64 eV, but the activation energy for rearrangement appears to be significant. Among the higher BICs isomerism has only been considered for B4I, for the arrangement of the two B_s atoms around the central $(B_2)_s$ dumbbell in a C_{2v} and in a C_2 geometry differs only by 0.35 eV in energy (in favour of the latter).

Table 3. LVMs of BICs calculated in the 64-atom supercell with the 2^3 MP set, 2NN shells around the BIC vibrating. Numbers set in roman and italic characters correspond to IR- and Raman-active modes, respectively, while bold denotes LVMs which are both IR- and Raman-active. Values above the phonon continuum are given for *isotopically pure* complexes of $^{11}B(^{10}B)$ in (cm^{-1}).

BIC			LVM	Frequency	LVM	Frequency
B_s^-	B^-	T_d	T_2 (IR/R)	**607(632)**		
B_i^+	BI^+	T_d		<520		
$(B_s + Si_i)^+$	BI^+	C_{1h}	A′ (IR/R)	**693(723)**		
$((B + Si)_s + Si_i)^-$	BI_2^-	C_{1h}	A′ (IR/R)	**671(698)**	A″ (IR/R)	**658(684)**
$(B_s)_2^0$	B_2^0	D_{3d}	A_{1g} (R)	*644(674)*	E_u (IR)	527(547)
$(B_s)_2^{2-}$	B_2^{2-}	D_{3d}	A_{1g} (R)	*627(657)*	E_u (IR)	577(602)
$(B_2)_s^0$	B_2I^0	D_{2d}	A_1 (R)	*1099(1152)*	E (IR, R)	**738(767)**
$(B_s–Si_i–B_s)^0$	B_2I^0	D_{3d}	A_{1g} (R)	*672(706)*	A_{2u} (IR)	882(908)
			E_g (R)	*586(608)*	E_u (IR)	604(628)
$(B_s–Si_i–B_s)^{2-}$	B_2I^{2-}	C_{1h}	A′ (IR/R)	**821(852)**	A″ (IR/R)	**719(748)**
				666(692)		**582(604)**
				573(594)		**569(589)**
$[(B_2)_s + Si_i]^0$	$B_2I_2^0$	C_{1h}	A′ (IR/R)	**926(969)**	A″ (IR/R)	**684(710)**
				565(585)		**539(560)**
$(B_s + B_i + B_s)^-$	B_3I^-	D_{3d}	A_{1g} (R)	*842(882)*	A_{2u} (IR)	1264(1326)
			E_g	*612(635)*	E_u	652(679)
$(B_s(B_2)_sB_s)^0$	B_4I^{2-}	C_2	A′ (IR/R)	**1095(1148)**	A″	**814(853)**
				729(763)		**637(663)**
				639(665)		
				566(589)		
				564(587)		
$(B_s(B_2)_sB_s)^0$	B_4I^{2-}	C_{2v}			A_1 (IR/R)	**1019(1068)**
					B_1 (IR/R)	**744(780)**
					B_2 (IR/R)	**730(759)**
			A_2 (R)	*641(667)*	B_2	**652(679)**
					A_1	**609(637)**

The LVMs of complexes with mixed isotopes have also been calculated and are given in table 4.

4. Comparison with available experiments

As mentioned before, the expected accuracy of the calculated vibration frequencies is about ± 30 cm^{-1}. (Note that modes with a higher degree of anharmonicity can be reproduced with even lower accuracy, due to the harmonic approximation. This is especially true for some BICs involving Si_i atoms.) Therefore, identification of experimentally observed vibrational centres with the models, based on the calculated values, can only be trusted if more than one mode of the centre is known and possibly the effect of isotope substitution has also been measured. Unfortunately, the available experimental information about the vibrations of BICs is scarce. The LVM of the isolated boron acceptor has been measured by both IR and Raman [24, 25] spectroscopy but further boron-related vibrations are only known from IR spectra of electron irradiated compensated samples [26–28]. (Compensation is necessary to get rid of the free carrier absorption which would mask the LVMs. In the case of neutron irradiation the created damage provides for compensation [29].) Matters are complicated by the presence of oxygen in Cz-Si samples which gives rise to a huge band between 1000 and 1100 cm^{-1} in the IR spectrum, making the observation of other features in this region extremely difficult. Based on

Table 4. LVMs of BICs calculated in the 64-atom supercell with the 2^3 MP set, 2NN shells around the BIC vibrating. Numbers set in roman and italic characters correspond to IR- and Raman-active modes, respectively, while bold denotes LVMs which are both IR- and Raman-active. Values above the phonon continuum are given for *isotopically mixed* complexes of ^{11}B (^{10}B) in (cm^{-1}).

BIC			LVM	Frequency	LVM	Frequency
$(B_s)_2^0$	B_2^0	C_{3v}	A_1 (IR/R)	**660**	E (IR/R)	**540**
$(B_s)_2^{2-}$	B_2^{2-}	C_{3v}	A_1 (IR/R)	**642**	E (IR/R)	**592**
$(B_2)_s^0$	B_2I^0	C_{2v}	A_1 (IR/R)	**1125**	B_1 (IR, R)	**738**
					B_2 (IR/R)	**767**
$(B_s–Si_i–B_s)^0$	B_2I^0	C_{3v}	A_1 (IR/R)	**688**	A_1 (IR/R)	**897**
			E (IR/R)	**592**	E (IR/R)	**622**
$(B_s–Si_i–B_s)^-$	B_2I^0	C_{1h}	A′ (IR/R)	**851**	A″ (IR/R)	**721**
				666		**593**
				588		**582**
$[(^{11}B–^{10}B)_s + Si_i]^0$	$B_2I_2^0$	C_{1h}	A′ (IR/R)	**941**	A″ (IR/R)	**696**
				585		**553**
$[(^{10}B–^{11}B)_s + Si_i]^0$	$B_2I_2^0$	C_{1h}	A′ (IR/R)	**954**	A″ (IR/R)	**699**
				565		**545**
$(^{11}B_s + ^{10}B_i + ^{11}B_s)^-$	B_3I^-	D_{3d}	A_{1g} (R)	*841*	A_{2u} (IR)	1304
			E_g	*613*	E_u	653
$(^{10}B_s + ^{11}B_i + ^{10}B_s)^-$	B_3I^-	D_{3d}	A_{1g} (R)	*882*	A_{2u} (IR)	1288
			E_g	*635*	E_u	678
$(^{11}B_s + ^{11}B_i + ^{10}B_s)^-$	B_3I^-	C_{3v}	A_1 (IR/R)	**861**	A_1 (IR/R)	**1277**
			E	**621**	E	**668**
$(^{10}B_s + ^{10}B_i + ^{11}B_s)^-$	B_3I^-	C_{3v}	A_1 (IR/R)	**862**	A_1 (IR/R)	1315
			E	**620**	E	669

circumstantial evidence (number of modes, splitting on isotope substitution, stability range) the boron-related centres in the IR spectrum (called P-, Q-, R- and S-lines) have been tentatively assigned to various models [26].

In table 5 we have compared the calculated LVMs of these models (in a charge state appropriate for compensated samples) with the observed data. The calculated frequency of the single acceptor, 607 cm^{-1} with an isotope shift of 25 cm^{-1}, against the observed 623 cm^{-1} with an isotope shift of 23 cm^{-1} marks the accuracy of the calculations. The R-line was assumed to originate from a complex of substitutional boron with one or more self-interstitials. At present we only have the LVMs of the $(B_s + Si_i)^+$, alias BI^+, and the $((B + Si)_s + Si_i)^-$, alias BI_2^- complex, at 693 (723) cm^{-1} and 671 (698) cm^{-1} for the isotope ^{11}B (^{10}B), respectively. The deviation from the observed 730 (757) cm^{-1} is not small enough in either case, to make the identification convincing based on just a single mode. The Q-line was assigned to interstitial boron [26] but Yamauchi *et al* suggested the $(B_2)_s$ complex (alias B_2I) instead, based on their calculations. Our result for the IR mode, 738 (767) cm^{-1}, is even closer to the experimental 733 (760) cm^{-1} but Raman measurements on Cz-Si would be needed to confirm the assignment by finding the high-frequency Raman-active mode.

In the case of the S-lines, with two known IR modes, the situation is more favourable. The suggestion of [26] was a complex of two boron atoms with trigonal symmetry. Since B_2 (i.e. $(B_s)_2$) has no high frequency modes the B_2I isomer with trigonal symmetry, $B_s + Si_i + B_s$ (suggested originally as a model for the I2 centre [30]), can be considered. The calculated IR modes, at 882 (908) and 604 (628) cm^{-1}, are reasonably close to the observed values 903 (928) and 599 (–) cm^{-1} for the isotopically pure complexes. Also the calculated modes for the mixed complexes, 897 and 622 cm^{-1}, fit the observed 917 and 603 cm^{-1}

Table 5. Comparison of early experiments on electron-irradiated compensated or neutron-irradiated material with calculated frequencies of those BICs which have been suggested as the origin of the observed vibrational centres. Only pure ^{11}B BICs are considered here. Numbers set in roman and italic characters correspond to IR- and Raman-active modes, respectively, while bold denotes LVMs which are both IR- and Raman-active. The I2 centre has been observed in photoluminescence.

Centre	Acceptor	R-lines	S-lines	Q-lines	P-lines	I2 centre
Stability range (°C)		<−40	−40 to −10	−10 to 220	Survives over 300	>200
Exptl. LVM	**623**	730	903	733	553	843
			599			242
References	[24, 25]	[26]	[26]	[26–29]	[26–29]	[30, 31]
Assignment	B_s^-	$B_s + nSi_i$	2B with trig. sym.	B_i	$(B_s)_2$	$2B_s + Si_i$, low sym.
Model	B_s^-	$(B_s + Si_i)^+$ $(B_s + 2Si_i)^-$	$B_s + Si_i + B_s$	$(B_2)_s$	$(B_s)_2$ or $(B_s)_2^{2-}$	
	T_2 **612**			A_1 *1026*	A_{1g} *585*	
(Theory) [12]				E **760**	E_g *603*	
					E_u 530	
Present	T_2 **607**	A_1 **693**	A_{2u} 882	A_1 *1099*	(0)/(2−)	A **821**
(theory)		A_1 **671**	A_{1g} *672*	E **738**	A_{1g} *644/627*	**719**
			E_u 604		E_u 527/577	**666**
			E_g *586*			**582**
						573
						569

agreeably. It should be noted, though, that the mixed complex has lower symmetry (no inversion) and the other two modes, which are Raman-active in the isotopically pure complex, should become visible in IR around 688 and 592 cm^{-1}.

From the boron-related centres in the IR spectrum (called P-, Q-, R- and S-lines), only the Q-line is stable at room temperature and only the P-line survives annealing up to 300 °C. The P-lines have been assigned to a pair of substitutional boron atoms [26]. Despite finding the $(B_s)_2$ complex metastable, Yamauchi *et al* [12] confirmed that the calculated IR-active mode of $(B_s)_2^0$, 530 cm^{-1}, is reasonably close to the experimentally observed 553 cm^{-1}. Our result for the IR mode, 527 cm^{-1}, is close to that of [12] (even though we only get one Raman-active mode, E_g, above the continuum with a frequency much higher than that of Yamauchi *et al*). We note, however, that in compensated samples the stable charge state should be $(B_s)_2^{2-}$, for which we obtain 577 (602) cm^{-1} for the isotopically pure complexes and 592 cm^{-1} for the mixed one. (Note that in the mixed complex an additional mode at around 642 cm^{-1} should become IR-visible.) The observed values, 553 (570) cm^{-1} for the pure and 560 cm^{-1} for the mixed complex, are still within the accuracy of the calculation. Additional support for the assignment stems from the report of a feature at 615 cm^{-1} correlating with the P-lines. This could be the mode (calculated at 642 cm^{-1}) which is only IR-active in the mixed complex. Still, a definite identification required knowledge of the corresponding Raman spectra.

In addition to IR centres, LVM assisted sidebands of the boron-related photoluminescence (PL) centre, called I2, has also been observed [30, 31]. Originally, this centre has been attributed to two boron and a self-interstitial atom with trigonal symmetry [30] but later a reduced symmetry was reported [31]. The calculated frequencies of the neutral B_2I (D_{3d}) isomer $(B_s–Si_i–B_s)^0$ obviously do not fit the modes of the I2 centre. The highest frequency of the dinegative (C_{1h}) isomer is, however, quite close to the observed I2 mode. Since we cannot, at present, calculate intensities, it is not clear why the other modes were not observed, if this complex is the origin of the I2 centre.

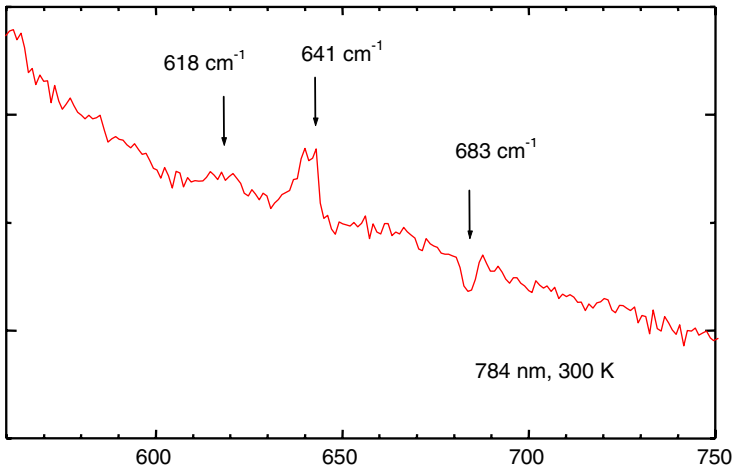

Figure 2. Difference of the Raman spectra in the low wavenumber region of two samples annealed at 900 °C for 30 min after $^{11}B^{+}$ implantation with doses of 10^{16} and 2×10^{15} cm^{-2}.

Parallel with the calculations, we have started IR/Raman investigation of silicon samples, heat-treated after high dose boron implantation. We present some preliminary results here. The Raman spectra taken after a 900 °C annealing showed several boron-related features. Figure 2 shows the difference spectrum of two samples implanted with ^{11}B doses of 10^{16} and 2×10^{15} cm^{-2}. Unfortunately, the level of compensation was not enough to distinguish LVM-related signals in the IR spectra.

The features at 618 and 683 cm^{-1} are present in both Raman spectra, the first increasing, the latter decreasing with the dose. Since the increasing implantation dose creates more damage and with that a stronger level of compensation, it is tempting to assign these two features to the Raman-active modes of $(B_s)_2^{2-}$ and $(B_s)_2^0$, with calculated frequencies at 627 and 647 cm^{-1}, respectively, assuming that increasing the level of compensation—and thereby raising the Fermi level—makes the former more, and the latter less, abundant. Electrical measurements on these samples as well as IR spectra are needed for confirmation of this suggestion. If it could be verified, it meant that the P-lines, i.e. the $(B_s)_2$ complex, could survive very high temperature annealing. Although this BIC is only metastable, it could be left behind as larger B_2I_m complexes lose the silicon self-interstitials. The redistribution of the B atoms into isolated substitutionals may require large activation energy. This process will also have to be investigated theoretically.

The feature at 641 cm^{-1} appears only in the sample implanted with the higher dose. Among the investigated complexes, $(B_2)_s + Si_i$, alias B_2I_2 has predicted LVMs in this region at 684 cm^{-1} (with additional ones at 565 and 539 cm^{-1}). The calculations also predict a higher mode at 926 cm^{-1}. Figure 3 shows the higher wavenumber part of the difference spectrum. (Note that, due to the huge oxygen peak in the spectra, the difference shows some artefacts denoted by asterisks.) As can be seen, there is indeed a broad band between 930 and 980 cm^{-1}. Obviously, further experimental studies on isotope effects, as well as investigation of compensated float zone samples, are needed.

5. Summary

Using *ab initio* supercell calculations we have calculated the LVMs of a large number of BICs in the harmonic approximation. Comparison with earlier data and those of new experiments

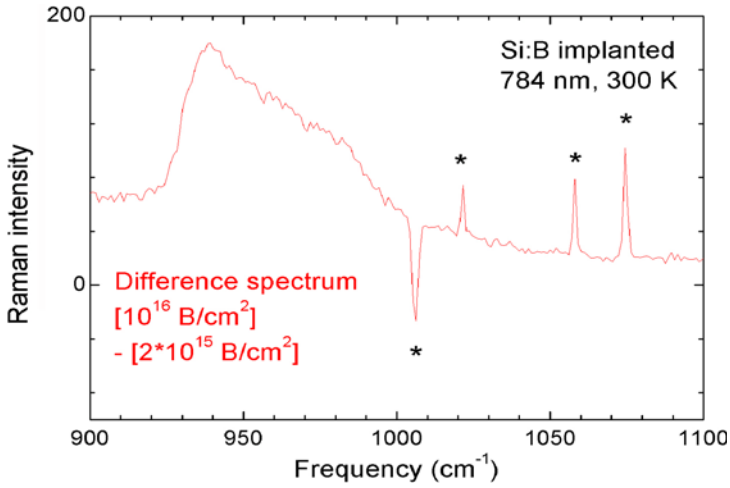

Figure 3. Difference of the Raman spectra in the high wavenumber region of two samples annealed at 900 °C for 30 min after $^{11}B^+$ implantation with doses of 10^{16} and 2×10^{15} cm^{-2}. Features marked by asterisks are artefacts of the subtraction in the range of the high oxygen peak.

promise the possibility of positive identification of the most important BICs at various stages of the annealing. Although not completely confirmed, the BICs identified so far are not the ones which played a key role in earlier kinetic simulations. Apparently, energetic stability is not the critical issue.

Acknowledgments

This work has been carried out in the framework of the EU FP5 IST-2000-30129 project 'FRENDTECH-EAST', using the resources of the supercomputer centres HLR Stuttgart, NISC Jülich and CINES Montpelier. Special thanks to the coordinator, Peter Pichler, for fruitful discussion and for initiating this work. We also appreciate his and Alain Claverie's help with the supercomputer grants.

References

[1] Pelaz L, Gilmer G H, Gossmann J-J and Raferty C S 1999 *Appl. Phys. Lett.* **74** 3657
[2] Caturla M J, Johnson M D and de la Rubia T D 1998 *Appl. Phys. Lett.* **72** 2736
Lenosky T J, Sadigh B, Theiss S K, Caturla M-J and de la Rubia T D 2000 *Appl. Phys. Lett.* **77** 1834
Zhu J, de la Rubia T D, Yang L H, Malhoit C and Gilmer G H 1996 *Phys. Rev.* B **64** 4741
Zhu J 1998 *Comput. Mater. Sci.* **12** 309
[3] Chakravarthi S and Dunham S T 2001 *J. Appl. Phys.* **89** 3650
[4] Windl W, Liu X-Y and Masquelier M P 2001 *Phys. Status Solidi* b **226** 37
Liu X-Y, Windl W and Masquelier M P 2000 *Appl. Phys. Lett.* **77** 2018
[5] Deák P 2003 *Computational Materials Science Proc. NATO ASI (Il Ciocco, Italy, Sept. 2001)* (Dordrecht: Kluwer–Academic) at press
[6] Sadigh B, Lenosky Th J, Theiss S K, Caturla M-J, de la Rubia T D and Foad M A 1999 *Phys. Rev. Lett.* **83** 4341
[7] Windl W, Bunea M M, Stumpf R, Dunham S T and Masquelier M P 1999 *Phys. Rev. Lett.* **83** 4345
[8] Hakala M, Puska M J and Nieminen R M 2000 *Phys. Rev.* B **61** 8155
[9] Pelaz L, Venezia V C, Gossmann J-J, Gilmer G H, Fiory A T, Jaraiz M and Barbolia J 1999 *Appl. Phys. Lett.* **75** 662
[10] Uematsu M 1998 *J. Appl. Phys.* **84** 4781

[11] Luo W-W and Clancy P 2001 *J. Appl. Phys.* **89** 1596
[12] Yamauchi J, Aoki N and Mizushima I 2001 *Phys. Rev.* B **63** 073202-1
[13] Smulders P J M, Boerma D O, Nielsen B B and Swanson M L 1990 *Nucl. Instrum. Methods* **45** 438
[14] Angress J F, Goodwin A R and Smith S D 1965 *Proc. R. Soc.* A **287** 64
[15] Harris R D, Newton J L and Watkins G D 1987 *Phys. Rev.* B **36** 1094
[16] Mizushima I, Watanabe M, Murakoshi A, Hotta M, Kashiwagui M and Yoshiki M 1993 *Appl. Phys. Lett.* **63** 373
[17] Okamoto M, Hashimoto K and Takayagi K 1997 *Appl. Phys. Lett.* **70** 978
[18] Artacho E, Sánchez-Portal D, Ordejón P, García A and Soler J M 1999 *Phys. Status Solidi* b **215** 809
[19] Troullier N and Martins J L 1991 *Phys. Rev.* B **43** 1993
[20] Kleinman L and Bylander D M 1982 *Phys. Rev. Lett.* **48** 1425
[21] Perdew J P, Burke K and Ernzerhof M 1997 *Phys. Rev.* B **77** 3865
Perdew J P, Burke K and Ernzerhof M 1997 *Phys. Rev.* B **78** 1396
[22] Monkhorst H J and Pack J K 1976 *Phys. Rev.* B **13** 5188
[23] Ögut S and Chelikowsky J R 1999 *Phys. Rev. Lett.* **83** 3512
[24] Smith S D and Angress J F 1963 *Phys. Lett.* **6** 131
[25] Chandrasekhar M, Chandrasekhar H R, Grimsditch M and Cardona M 1980 *Phys. Rev.* B **22** 4825
[26] Tipping A K and Newman R C 1987 *Semicond. Sci. Technol.* **2** 389
[27] Newman R C and Smith R S 1967 *Phys. Lett.* A **24** 671
[28] Bean R S, Morrison S R, Newman R C and Smith R S 1972 *J. Phys. C: Solid State Phys.* **5** 379
[29] Laithwaite K, Newman R C and Totterdell D H J 1975 *J. Phys. C: Solid State Phys.* **8** 236
[30] Thonke K, Weber J, Wagner J and Sauer R 1983 *Physica* B **116** 252
[31] Thonke K, Bürger N, Watkins G D and Sauer R 1984 *Proc. 13th Int. Conf. on Defects in Semicond.* p 823